Ecological Engineering 130 (2019) 271–281

Contents lists available at ScienceDirect

Ecological Engineering

journal homepage: www.elsevier.com/locate/ecoleng

Wave dissipation across a *Rhizophora* mangrove patch on a Colombian Caribbean Island: An experimental approach

Catalina A. Vanegas G[a,*], Andres F. Osorio[a], Ligia E. Urrego[b]

[a] OCEANICOS Research Group, Escuela de Geociencias y Medio Ambiente, Universidad Nacional de Colombia, Sede Medellín, Medellín, Colombia
[b] OCEANICOS Research Group, Departamento de Ciencias Forestales, Universidad Nacional de Colombia, Sede Medellín, Medellín, Colombia

ARTICLE INFO

Article history:
Received 31 January 2017
Received in revised form 5 July 2017
Accepted 7 July 2017
Available online 15 July 2017

Keywords:
Effective vegetation length scale
Drag coefficient
Reynolds number
Wave dissipation by vegetation
Energy flux

ABSTRACT

Coastal ecosystems like coral barrier reefs and mangrove forests have been designated as environments in need of protection. This is not only because they are threatened by climate change, but also because of the important role they play in coastal protection. Some field studies based on *Rhizophora* mangrove trees have analyzed the force induced by water flow over their roots and the wave dissipation capacity of these trees under tidal regimes and sea waves. Various methods have been used to calculate energy dissipation in the past, but these do not include the drag coefficient (C_D) with field data calibration. The study presented here was conducted to investigate the capacity of a small natural *Rhizophora* mangrove patch (at experimental scale) located on Isla Grande in the Colombian Caribbean Sea to mitigate wave energy. The total energy dissipation, including the slope bottom and the effects of vegetation, was calculated. Parametric equations were used to calculate the effects of vegetation. The drag force (F_D) was computed using Morrison's equation and the C_D was calculated using Mazda's method. The results show a mean energy dissipation difference of 9.6% between the energy balance and dissipation coefficients where the C_D was calculated for each sea state. The dissipation coefficients were calculated with constant C_D values (0.06, 3.48 and 6.90). None of the three cases could explain the 90.4% energy flux, as in the case of vegetation dissipation (D_{veg}) with calculated and non-constant C_D values. Despite the small size of the mangrove patch, the results show an increase in the C_D (with values of up to 7.9) as a result of lower values of the Reynolds number (R_e) (about 7.3×10^5). This demonstrates experimentally the role that even a small patch of mangrove vegetation plays in attenuating sea waves (as C_D is a function of sea states), and higher magnitudes were obtained than those recorded in the literature using other vegetation types. A nonlinear contribution to energy flow by bottom dissipation and vegetation dissipation was observed. Our results highlight the need to scale measurements up to forest level in order to accurately quantify the impact of mangrove vegetation on wave attenuation and determine the possible impact on the protection of coastal ecosystems and infrastructure.

1. Introduction

Mangroves provide widely recognized ecological benefits such as shoreline stabilization, inland structure protection (Lewis, 2005) and climate change mitigation. They play a structural and functional role in the stability of the coastline (Robertson and Alongi 1992; Yáñez-Arancibia et al., 2010) and hydrodynamic force attenuation. In turn, hydrodynamics, and morphological, bathymetric and climatic conditions influence the structure, growth, distribution and dominance of different plant species across the intertidal zone (Jimenez, 1980; Suárez et al., 2015). Mangrove forests are being taken into account for the development of coastal management tools in different tropical contexts (Aswani et al., 2012). To support these management practices, it is imperative to have specific knowledge on ocean and wave dynamics, sediment flows, coastal geomorphology, mangrove vegetation structure and propagule dispersion distance (Lewis, 2005). Knowledge of quantitative data for swamp hydrodynamics would also be an important tool to support mangrove conservation (Mazda, 2014) and management.

Regarding the hydrodynamics and hydraulic resistance of coastal vegetation (e.g. mangrove forests, saltmarshes, wetlands, etc.), some studies have pointed out that vegetation dissipates wave energy and can be a natural barrier against extreme events (Husrin

* Corresponding author at: Universidad Nacional de Colombia, Sede Medellin,Carrera 80N°65-223 (Bloque M2). Medellín, Colombia. Tel.: +57 4 2977883; Fax: +57 4 4309018.
E-mail address: cavanegasg@unal.edu.co (C.A. Vanegas G).

https://doi.org/10.1016/j.ecoleng.2017.07.014
0925-8574/

and Oumeraci, 2009). However, Chatenoux et al. (2005) suggest that vegetation structures do not always effectively protect coastal areas from destruction by extreme events such as tsunamis because their wave dynamics have different magnitudes and directions than normal wind waves. However, hardly any accurate measurements of the vegetation structural parameters are included in their physical parameter calculations. Therefore, there is an opportunity to research the properties involved in this kind of coastal protection, such as vegetation roughness, wave turbulence, and drag and inertia forces, among other factors. In this context, the resistance of vegetation to extreme and mean incident sea waves has been studied in laboratory experiments, numerical simulations and field data analysis (Mazda et al., 1997a, 1997b; Husrin and Oumeraci, 2009; Maza et al., 2015).

The interaction of vegetation and waves is complex due to the spatial variability of vegetation density and geometry (Ozeren et al., 2009) and the configuration of the *Rhizophora* prop roots, the species most widely studied as a wave dissipater. In the complex prop root structures, the ratio between the variable submerged root volume and frontal tree areas influences the drag force under steady flow conditions (Husrin et al., 2012).

A mangrove geometric approximation is advantageous because it uses different equations to calculate the resistance of a forest to wave energy. In this way, several numerical simulations using vegetation field data have been employed to predict the wave dissipation term based on a nonlinear formulation of the drag force, using linear wave theory (Dalrymple and Dean, 1984; Mazda et al., 1997b; Mendez and Losada, 2004) and shallow water equation models, or Boussinesq equations. These neglect inertia forces and ignore the apparent bottom friction, but use the conservation of momentum approach instead (Ozeren et al., 2009). In addition, these models are based on energy flux and make a linear superposition with the dissipation terms generated by different agents that affect the flux.

Based on field data, physical schemes using an array of cylinders to represent the structural features of coastal vegetation have been implemented in different experiments to evaluate wave attenuation as a function of vegetation type, root density, and height. Incident wave conditions like breaking or non-breaking zones using a coastal vegetation macro roughness approach have also been investigated (Ozeren et al., 2009). Some experiments used materials that artificially simulate vegetation stiffness, such as flexible or rigid cylinders (Augustin et al., 2009; Ozeren et al., 2009; Hui et al., 2010; Huang et al., 2011; Noarayanan et al., 2012; Hu et al., 2014a).

The hydraulic resistance of natural structures such as trees can be described using drag, inertia, and Manning coefficients, and/or field data correlations to R_e (Booij et al., 1999; Mazda et al., 1997b; Anderson et al., 2011). In particular, drag and inertia coefficients are highly influenced by the geometrical characteristics of the trees and roots. However, prop root density and distribution contribute to wave dissipation and increase the calculated drag coefficient (C_D), which also affects the water surface slope (Iimura and Tanaka, 2012). Previous studies have not included an analysis of the C_D for each sea state to calculate the dissipation across a mangrove forest.

In particular, the experimental results of Ozeren et al. (2009) show the differences in C_D among rigid and flexible cylinders representing vegetation and live vegetation models. In the latter case, C_D depends on the variations in relative tree height and the related tree diameter to determine the geometric and physical properties of live vegetation. In the same way, Hu et al. (2014) present C_D calibrations for different interactions of wave currents with submerged and emergent vegetation models. The findings of Ozeren et al. (2009) and Hu et al. (2014) suggest that in the flooding phase the way wetlands attenuate wave energy may be critical for coastal protection practices.

The question remains as to how we can find a real C_D value to determine dissipation caused by the vegetation field in mean wave conditions, as a first approximation. In this work, field data was collected from a small patch of *Rhizophora mangle* to calibrate the C_D in relation to sea state. Using this information, we analyzed agents that affect energy flux, such as dissipation associated to the vegetation structure, using the Mendez and Losada (2004) approximation and the bottom or breaking dissipation equation (Alsina and Baldock, 2007). Mendez and Losada (2004) developed an empirical model for wave transformation over a vegetation field, based on a nonlinear formulation of F_D with a calibrated value of C_D for a specific type of plant. This paper is organized as follows: Section 2 presents the implemented methodology and the equations used, a description of the study site, and the data measured. Section 3 gives a description of the results obtained for the energy dissipation values and the drag coefficient. The last section gives the final discussion and conclusions.

2. Methods

2.1. Theoretical framework

To determine the percentage of wave height reduction when waves cross the vegetation, the energy dissipation was calculated based on the conservation of energy flux between several points and the linear sum of dissipation coefficients according to vegetation and bottom or breaking effects. Due to the difficulty in determining the contribution of all physical processes, the linear addition of dissipation coefficients assumed by Mendez and Losada (2004) was used as a good approximation to describe the wave energy transformation over a vegetation stand whenever the C_D value had been previously calibrated. These coefficients are parametric and nonlinear functions that allow the theoretical comparison and predominance of one or more physical process when calculating energy flux and determining the nonlinear interactions related to these processes. Eqs. (1) and (2) represent the energy flux as a function of the wave energy equation.

$$\frac{\partial EC_g}{\partial x} = D \tag{1}$$

$$\frac{1}{8}\rho g \frac{\partial C_g H^2}{\partial x} = D_{veg} + D_{slope} \tag{2}$$

Where E is wave energy, g is the gravitational acceleration, $\frac{\partial C_g}{\partial x}$ is the difference in the speed at which wave energy travels, ρ is the water density, H is the wave height representative of the random wave field and D represents the dissipation of wave energy as a sum of dissipation caused by different physical processes. In the present study, the dissipation processes evaluated were vegetation (D_{veg}) (Mendez and Losada, 2004) and wave breaking (D_{slope}) (Alsina and Baldock, 2007). Although other physical processes like refraction, reflection and shoaling may be important, Mendez and Losada (2004) do not consider the reflection induced by plants in their proposed empirical model as it has a very low effect on wave energy. Shoaling effects are canceled out by the energy dissipation induced by the vegetation as wave height increases. In their field studies, Horstman et al. (2014) found values of H_s between 0.0 m and 0.15 m, noting that the wave reflection might increase for high incident waves and have low values for low waves. They also obtained shoaling rates one order of magnitude smaller than the attenuation rates. Thus, these effects were not quantified in the present work.

To use Eq. (2), we considered that the predominance of energy transfer is in the direction of the beach. In this way, the negative values represent offshore fluxes due to reflection and mangrove vegetation effects.

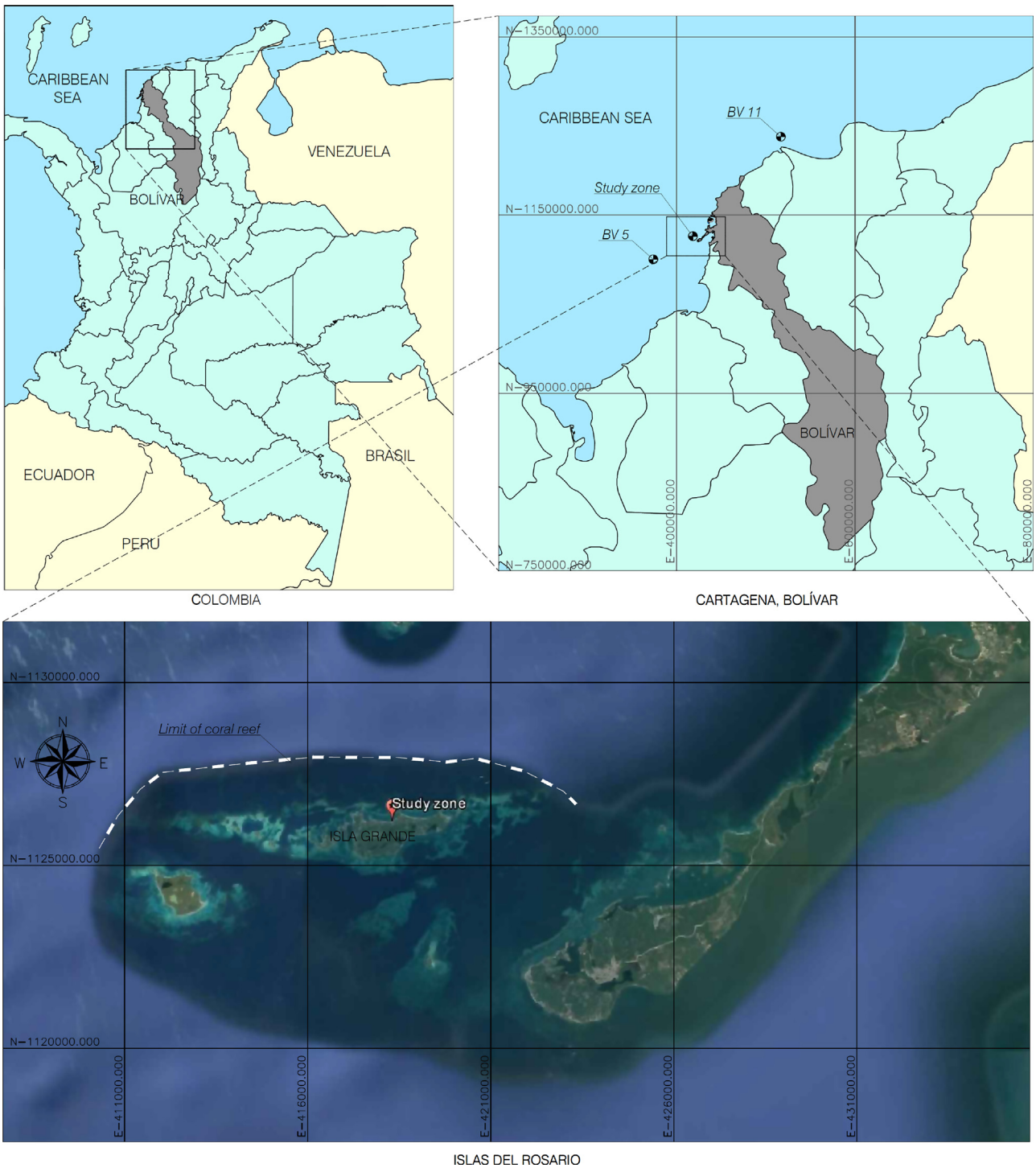

Fig. 1. Location of the study site (UTM coordinates).

Mendez and Losada (2004) present a nonlinear approximation (Eq. (3)) to calculate wave dissipation over an experimental vegetated zone, where N is the vegetation density in cylinders per square meter, d the mean root diameter, C_D the drag coefficient (suggested by authors to be 1 for trees including mangroves), k is the wave number, ω the angular frequency, h the water depth (locally constant), α the water fraction occupied by the vegetation (assumed by the authors to be 1 for emerged vegetation).

$$D_{veg} = \frac{1}{2\sqrt{\pi}}\rho N d C_D \left(\frac{kg}{2\omega}\right)^3 \frac{sinh^3(k\alpha h) + 3sinh(k\alpha h)}{3kcosh^3(kh)} H^3 \quad (3)$$

However, to implement equation 3 in this study, some considerations were taken into account. First, in accordance with Husrin and Oumeraci (2009) and Mazda et al. (1997b), values of C_D higher than 1 were used. The drag coefficient values were calculated by Mazda's method for each sea state measured in the field. Second, due to the beach profile being sloped between the control points, the value of h was adjusted over each point according to the depth measured in the field (Fig. 2). Finally, as not all the roots of the mangrove patch had emerged, the value of α used was 0.8. These considerations are based on Mendez and Losada's (2004) results. The vegetation affects the bottom dissipation because the reduced

wave height generates a decrease in the *H/h* ratio, thereby inducing wave breaking.

The dissipation caused by wave breaking was calculated with the modified Battjes and Janssen (1978) equation seen in Alsina and Baldock (2007) (Eq. (4)), where the ratio $H/h \neq 1$. This is a parametric equation that takes into account the nonlinear behavior of the flux and is calibrated and validated with laboratory data and numeric models using variable bathymetry. *A* is a sediment factor calculated by Eq. (5), f_p is the peak frequency and *B* is an adjusted parameter of measured data. *erf* is the Gauss error function that is programmed by default in the *math* package in the programming language *python*, H_b is the maximum wave height before the break and it is a function of wave number. *H* is the significant wave height and γ is the parameter calculated with its initial wave height and length (see Eqs. (6) and (7)).

$$D_{slope} = A\frac{H^3}{h}\left[\left(\left(\frac{H_b}{H}\right)^3 + \frac{3H_b}{2H}\right) exp\left(> \left(\frac{H_b}{H}\right)^2\right) + \frac{3\sqrt{\pi}}{4}\left(1 > erf\left(\frac{H_b}{H}\right)\right)\right] \quad (I4)$$

$$A = \frac{1}{4}\rho g f_p B \quad (5)$$

$$H_b = \frac{0.88}{k} tanh\left(\gamma\frac{kh}{0.88}\right) \quad (6)$$

$$\gamma = 0.5 + 0.4 tanh\left(33\frac{H_0}{l_0}\right) \quad (7)$$

In contrast with vegetation dissipation equations, for wave breaking dissipation equations the empirical parameter was used with values suggested by the authors.

In this way, to obtain C_D values, the total force (F) for the waves was calculated by means of the Morison equation (Morison et al., 1950), where F_D and F_M are the drag and inertia forces, respectively, C_D and C_M are the corresponding coefficients, and ρ is the water pressure. A is the cross-sectional area facing the flow on a vertical plain, V is the object volume, u is the flow velocity and $\frac{\delta u}{\delta t}$ is the flow acceleration.

$$F = F_D + F_M = \frac{1}{2}C_D\rho A u|u| + C_M\rho V\frac{\delta u}{\delta t} \quad (8)$$

To implement Eq. (8), we assumed F_M to be small compared to F_D due to the small relative diameters of the tree roots compared to the water depth, which is typical of wave interaction with small bodies and a steady flow. Thus, with relatively high waves F_M is typically neglected (Dalrymple et al., 1984; Mendez and Losada, 2004). Total horizontal force using the Morrison equation without the inertia component is a function of F_D.

Also, the momentum balance was written as in equation 9, where η is the water free surface and $> g\frac{\delta\eta}{\delta x}$ is the water pressure over point x. F is the flow resistance (Eq. (8)) where the bottom friction can be neglected in densely vegetated zones. Thus, F becomes a function of F_D calculated by the expression $\left(\frac{1}{2}C_D\rho A u|u|\right)$, where *u* should be the relative velocity between the fluid and plant. However, Mendez and Losada (2004) took *u* as the incident wave velocity for rigid and flexible plants considering a different value of C_D to cover the unknown plant motion.

Both terms on the right side of the equation represent the hydrodynamic behavior of the sea waves over water volume as a function of the area in front of the wave direction and the submerged depth. These terms were integrated into the water volume, with *I* as the water surface gradient and L_e as the effective vegetation length scale (Eq. (11)) (Mazda et al., 1997b). This methodology for mangrove swamps involved a depth-averaged momentum equation, and neglected both acceleration terms on the left side of Eq. (9) (Mazda et al., 1997b). These terms are one or two orders of magnitude smaller than the surface gradient. In this way, C_D was calculated as is presented in Eq. (10).

$$\frac{\delta u}{\delta t} + u\frac{\delta u}{\delta x} => g\frac{\delta\eta}{\delta x} + F \quad (9)$$

$$C_D = \frac{2gI}{u^2}L_e \quad (10)$$

$$L_e = \frac{V > V_m}{A} \quad (11)$$

The effective vegetation length scale (Eq. (11)) is a geometric characteristic of the studied patch. It is calculated as the ratio of the difference between *V* (water volume) and V_m (root volume) and *A* (projected area perpendicular to flow direction). This difference was obtained by subtracting the volume occupied by the vegetation structures in the water (i.e. the volume of the roots and the trunk) from the control water volume (Husrin and Oumeraci, 2009; Mazda et al., 1997b). This parameter included essential information about the mean root density and mangrove patch size.

Due to the complexity of the problem, to use equation 10 the incident velocity was calculated based on the free wave surface measurements, as it was easy to collect wave height data within the vegetation patch. In this way, the wave-free surface measurements taken from sensors located in front of the mangrove patch were used to obtain a spectral velocity ($\int u$) approximation using the linear theory (Svendsen 2006). The use in this work of the linear wave theory in a near shore system is considered valid by several authors (Dalrymple and Dean, 1984; Mendez and Losada, 2004; Vo-Luong and Massel, 2008) and can be utilized as a first approximation to calculate the drag force per sea state over a mangrove patch. The spectral density of pressure ($\int P$) can be calculated with the information recorded by the installed sensors as a function of the spectral free-surface ($\int \eta$). However, the spectral velocity is also a function of the spectral free-surface, including the group celerity in terms of angular frequency (ω) and wave number (k) (Svendsen, 2006). An expression to calculate the spectral velocity in terms of the spectral free-surface and celerity group was derived from the spectral free-surface using the linear theory (Eq. (12)). The velocity of each sea state was then calculated as a function of the zero order moment of the velocity spectrum.

$$\int u = \omega^2\left(\frac{\cosh kh}{\sinh kh}\right)^2\int P \quad (12)$$

Additionally, to differentiate the effect of the vegetation from the effect of the bottom, the PETRA model (*Modelo de Evolución de PErfil TRAnsversal*) was used. This model is one of the SMC (*Sistema de Modelado Costero*) options (González et al., 2004), where the Battjes and Janssen, (1978) linear theory was used to calculate the evolution of significant wave height across a bathymetric profile related to bottom dissipation. The model was fed with the boundary conditions provided by the data measured at WG3, located in front of the mangrove patch, and the values of H_s were calculated at locations WG2 and WG1 (Fig. 2). The results obtained with the PETRA model were compared with the measurements taken to show the difference between, firstly, break dissipation by the bathymetric profile, and secondly, the combined effect of vegetation and breaking.

2.2. Study site

In order to validate the theory of the Morrison equation and apply methodologies that explain dissipation by vegetation, a mangrove patch of 26.26 m^2 was chosen. This allowed measurements to be made of the water surface inside, in front of and behind it. In addition, the small size of this patch allowed us to measure the

variability of root diameters and trunks of the trees as well as the number and height of submerged roots. The patch is formed by 3 *R. mangle* trees that were divided into four quadrants to measure the geometry. This small sample of mangrove forest was used experimentally to analyze the resistance of the *R .mangle* patch to sea waves and tides. It could be used as a first approximation to calculate mangrove dissipation and forces because it allowed controlled measurements to be taken of mangrove roots and incident sea waves.

Isla Grande is one of the 30 islands located in the Islas del Rosario archipelago, 35 km southwest of Cartagena in the Colombian Caribbean. On the northern part of the island, there are several vegetation patches of *R. mangle* facing the incident sea waves. Before their arrival to the mangrove patches, these waves cross over a coral barrier reef that surrounds the islands. The 26.26 m^2 patch is situated at lat = 419132<lon = 1125450 (UTM) (see Fig. 1). In general, the climatic seasonality is typical of the southern part of the Caribbean Sea and is caused by oscillations of the Inter-Tropical Convergence Zone (ITCZ) (Osorio et al., 2016). Caribbean coasts are dominated by wind waves produced locally and their intensity depends on the dry or wet seasons. A general description of sea waves on the Islas del Rosario archipelago was based on Osorio et al. (2016). We used the description of the general conditions of wave climate from the *Gulf of Morrosquillo virtual buoy (BV 5)*.

This buoy is localized about 51 km from the study site, where the most frequent sea states are north-easterly to northerly with values of significant wave height of less than 1.2 m. The most energetic components are toward southeast with average Hs values of around 2.0 m and a peak period of 8 s (Osorio et al., 2016). The sea wave behavior in the study zone is associated with the clockwise gyre of trade winds along the Caribbean Coast.

The field data was collected during the wet season, from May<November. This season is characterized by the highest precipitation (a monthly average of 125.7 mm) and relatively weak winds that blow from north to south until August. Osorio et al. (2016) show H_s values in May between 1.2 m and 2.0 m at *BV 11(Barranquilla virtual buoy)* and 0.7 m<1.2 m at *BV 5*, and Tp values from 6.9 s to 8.0 s and 6.2 s<8.2 s respectively.

2.3. Measurements

To evaluate wave dissipation by the mangrove patch, the field data collected was divided into two components. The first corresponds to the geometric characterization of the root mass taken using quadrants, a caliper, measuring tape and GPS. The second corresponds to the hydrodynamic measurements made using the layout of three wave gauges (WG) that cross the mangrove patch and are perpendicular to the sea wave direction. These WGs were located with reference to WG1, where the depth during the days of measurement was partially constant.

In order to obtain information about the mangrove patch, a pre-sampling statistical method was used (LEMA, 2003). The change in root distribution, density and diameters of the trees with depth was measured using a PVC quadrant with an internal area of 1.06 m for 4 representative zones of the mangrove patch. The equation for this method is presented below (Eq. (13)), where m is the required number of quadrants, t is the value of the t-student distribution for an error e of 15%, σ is the variance (1.5) as a relationship between the mean basal area (5.3 cm^2) of the roots and the standard deviation (7.9) and n is the data number (the number of roots).

$$m = \frac{t^2\sigma^2}{e^2 + \frac{t^2\sigma^2}{n}} \tag{13}$$

In each zone, the quadrant was placed arbitrarily about 1.2 m above the sea floor, and the number of roots, mean root diameters (emergent and submerged), and mean flood depth in the middle of the quadrant were measured. A summary of the data collected is shown in Table 1.

With the information from the four quadrants, the minimum number of quadrants was calculated using the pre-sampling equation (Eq. (13)). With the t-student distribution, this number is 3.7. This means that the 4 zones selected and measured cover the variability of mangrove roots in the vegetation patch. With the information collected, the characteristic length Le of the patch was obtained. These results are shown in Table 1.

In order to measure the water elevations at sites WG1<WG3, wave pressure gauges were placed and measurements were continuously recorded over 57 h, from 8 to 10 May 2014 during the wet season in the Caribbean Sea, i.e. when the wave energy is lower.

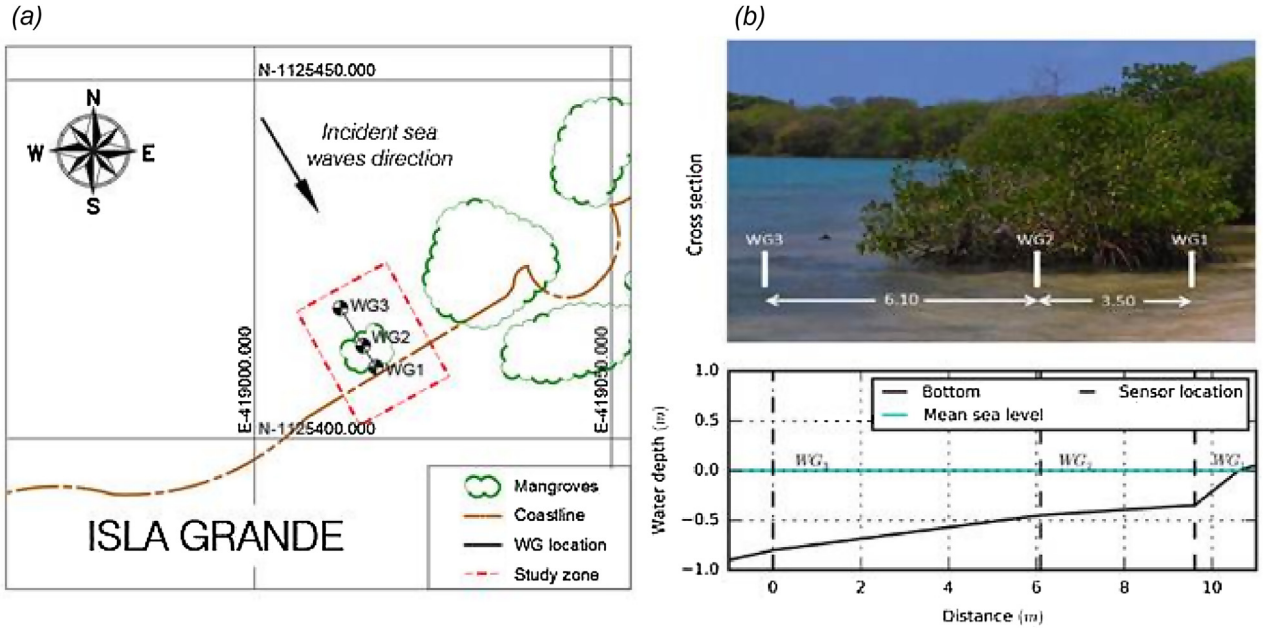

Fig. 2. Location of wave gauges at the study site. (a) Plan view (b) Cross section.

Table 1
Mangrove data collected. *Q* is the number of the quadrant, *n* the number of measured roots, d the mean diameter per quadrant, *h* the water depth in the middle of the quadrant, V_m the volume of the submerged roots calculated using the measured root diameter (not with the mean value), *V* the control volume, *A* the projected area per quadrant facing the flow direction and L_e the effective vegetation length scale (Eq. (13)).

Q	n	d (cm)	h (cm)	Vm (cm^3)	V (cm^3)	A (cm^2)	L_e (cm)
1	42	1.9	45	3731	505620	4770	105.2
2	38	2.2	48	3926	539328	5088	105.2
3	9	3.2	56	1612	629216	5936	105.7
4	8	1.9	38	574	426968	4028	105.9

Data was taken with a 1 Hz interval. The first wave gauge (WG) was located behind the mangrove patch at a water depth of 0.35 m and at a distance of about 1.0 m from the shoreline. The second WG was located 3.50 m from the first one but in front of the denser mass of roots and at a water depth of 0.46 m. The last gauge was located 6.10 m from the second one and at a water depth of 0.85 m (Fig. 2).

To analyze the data collected and calculate the significant wave height and the peak period, the data was grouped by 1-h sea states. The spectral analysis included the first 2048 data values and a Fast Fourier Transformation (FFT) routine. Depth correction for the pressure signal due to sensor location was carried out. These values were recorded in the broken wave zone, where the energy is lower than in the breaking and pre-breaking zones (in deep waters before the coral reef limit) due to the location of the mangrove patch behind the coral reef, as shown in Fig. 1.

To calculate the wave dissipation in the mangrove patch and the drag force using Eqs. (1)<(5), the C_D needed to be calculated. Mazda et al. (1997b) developed a methodology for tidal scale measurements, where the momentum equation is reduced to a balance between the water surface slope and the F_D. In mangroves, the tidal flow is considered to be dominant in a direction perpendicular to the tidal creek. This is due to the larger tidal wave length compared to the creek length. In our case, the incident flow direction is also perpendicular to the vegetation patch and the wavelength is higher than the vegetation length. The wavelength (as a periodic function in shallow water) calculated using the information recorded in WG3 is greater than the size of the mangrove patch in 60% of the measured sea states. In addition, the incident wavelength is greater than the mangrove patch size in 56% and 74% of the time series, using the information of the WG2 and WG1 gauges respectively. In this way, at the 3 sensors the measured wavelengths are higher than the mangrove patch size 50% of time. Hence, for an approximation of the tidal scale, the use of Mazda's methodology can be assumed and supported.

The Mazda et al. (1997b) method was implemented by employing the significant wave height for each sea state behind and in front of the mangrove patch, using Eqs. (9)<(11) at the same time, where I is the water surface gradient, calculated as the difference in Hs between WG 2 and WG 1. The incident velocity was obtained using the data recorded in WG3 and Eq. (12). The R_e was calculated using Eq. (14) to determine the conditions of the incident flow. The ratio between R_e and C_D has previously been used to relate the flow regime to vegetation response (Mazda et al., 1997b; Husrin and Oumeraci, 2009).

$$R_e = \frac{L_e u}{\upsilon} \tag{14}$$

The total energy dissipated by the break and vegetation coefficients was calculated and compared with the energy flux for 2 known sensors (WG1 and WG2). This comparison is useful to determine the unknown energy dissipation that may represent other interaction processes in the study zone due to the relationship between vegetation, waves and the bottom. The energy flux was calculated using Eq. (15). The wave dissipation across the mangrove patch was calculated by comparing the flux energy dissipation (Eq. (15)) with the dissipation obtained from parameterizations as the sum of equation 3 plus Eq. (4).

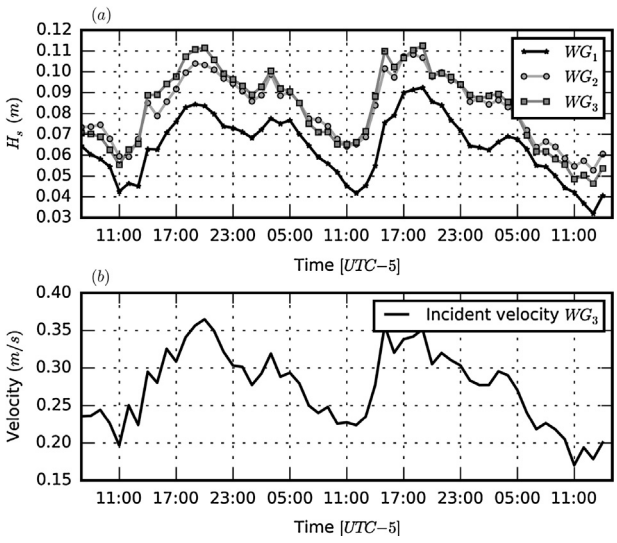

Fig. 3. (a) H_s from 7:00 on May 8<16:00 on May 11, 2014. (b) Wave velocity (Svendsen 2006).

$$\frac{(EC_g)_2 > (EC_g)_1}{\Delta x} = D_{2>1} \tag{15}$$

Similarly, as is shown in Fig. 2, it is important to note that the study area can be divided into two different zones. The first zone is located between WG3 and WG2 (from 0.0 m to 6.10 m) and the second zone is between WG2 and WG1 (from 6.10 m to 3.50 m). In both zones there are many dissipation processes, such as the effects of refraction, shoaling, breaking and vegetation. However, in the second one, where the mangrove patch is located, the wave dissipation is more influenced by the effect of vegetation. Therefore, the comparison shown by Eq. (15) can be made only with sensors WG2<WG1, because they delimited the mangrove zone. Meanwhile, in the zone between sensors WG3<WG2, other dissipation processes occur and vegetation processes are not predominant.

3. Results

As shown in Fig. 2, the WGs were placed along a transect at sites 1<3. WG1 was located behind the mangrove patch, WG2 was located in front of the denser mass of mangrove trees, and WG3 was aligned with the other sensors 6.10 m away from WG2. The waves moved from WG3 to WG1 and the significant wave height (H_s) is shown in Fig. 3. The significant wave height peak values were measured during the night and the non-peak values were measured in the morning, in accordance with the tidal regimen. Fig. 3 also shows the daily unimodal behavior of the Hs. The mean values are around 0.06 m at WG1, 0.08 m at WG2 and 0.09 m at WG3.

The wave velocity calculated from the data measured at WG3 is presented in Fig. 3(b). This wave velocity behavior is similar to the H_s values recorded at the same site, with mean and maximum values of 0.27 m/s and 0.36 m/s respectively. On the other hand, Fig. 4(a) presents the drag force F_D calculated with the methods of Morrison (Eq. (8)) and Mazda (Eq. (9)). The F_D calculated with the R_e changes according to the sea state and reaches values between 14.0 N and 88.0 N, with a mean value of 52.9 N. Fig. 4(b) and (c) show the behavior of C_D calculated for each sea state vs the R_e number, with values between 0.8 and 8.0. Fig. 4(b) is shown as constant values, using three C_D values suggested in the literature (Mendez and Losada, 2004; Husrin and Oumeraci, 2009). Therefore, the C_D

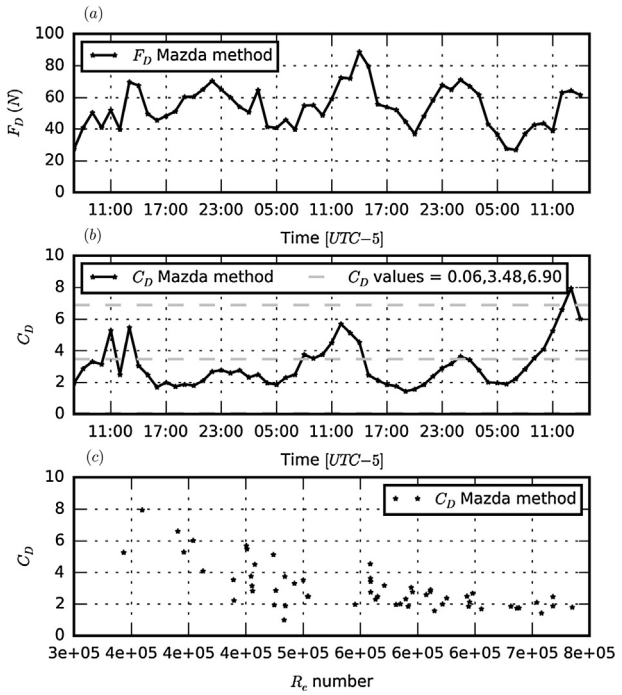

Fig. 4. (a) F_D per sea state (N). (b) C_D per sea state. (C) C_D as a function of the Reynolds number.

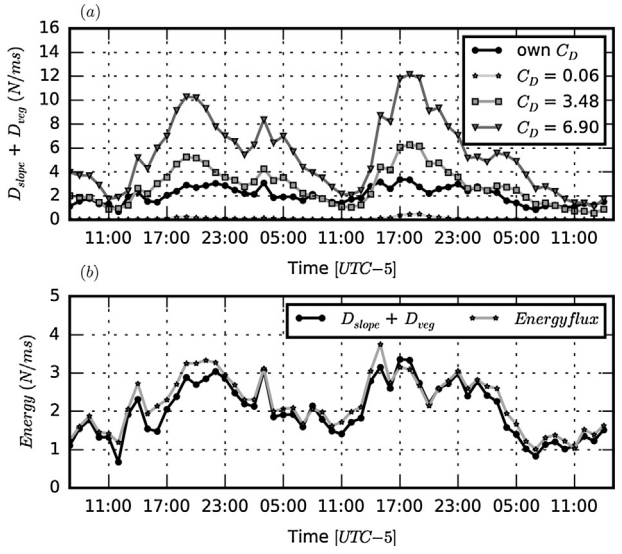

Fig. 5. Wave dissipation. (a) Breaking and vegetation dissipation with several C_D values (N/ms) (Eq. (3) + Eq. (4) in WG 2 + WG1). (b) Energy flux vs breaking and vegetation dissipation with our C_D values (N/ms) (Eq. (15) vs Eq. (3) + Eq. (4) in WG 2 + WG1).

values are variable as a function of H_s and T_p as sea state parameters. These values were used to calculate dissipation by vegetation. In the last part of Fig. 4, the highest values of C_D are presented when R_e reaches its lowest values. A comparison of results is shown in Fig. 5.

To calculate the linear sum of D_{veg} and D_{slope} of both sensors (WG1 and WG2), we used the values of C_D (0.06, 3.48 and 6.90) suggested in the literature for all sea states per sensor. These results were compared with the same values calculated with the C_D obtained in this work, as a function of sea state (Fig. 5(a)). This comparison shows a $D_{veg} + D_{slope}$ mean difference of 1.93 N/ms, 1.49 N/ms and 4.91 N/ms between the values calculated with the C_D shown in Fig. 4(c) and those calculated with the constant C_D, respectively. The behavior of the dissipation coefficients underestimates the dissipation using $C_D = 0.06$ and overestimates the dissipation using $C_D = 3.48$ and $C_D = 6.90$.

In addition, the wave dissipation across the mangrove patch in the study zone was calculated using the linear sum of breaking and dissipation by vegetation at sensors WG2 and WG1, where the physical processes that dominate the energy flux behavior are those related with mangrove patch dissipation and bottom friction. The final dissipation in the small grid was compared with the energy flux between WG2<WG1 using equation 15. The wave dissipation results shown in Fig. 5(b) have an approximation percentage of 90.4%, which explains the similarity between the calculated coefficients and the dissipation of energy flows recorded by direct measurements. The approximation percentage demonstrates a good approach to evaluating energy flux using the C_D values calculated for each sea state. The remaining percentage (9.6%) may represent physical processes such as refraction and shoaling, which are a product of the vegetation-wave-bottom interaction. As shown before, these processes have the lowest values of all the dissipation processes and have lower values than dissipation by breaking and vegetation (Mendez and Losada, 2004; Horstman et al., 2014).

Finally, to differentiate the evolution of H_s due to the interaction of the vegetation and bottom from the evolution of H_s caused only by the bottom, the PETRA model was used. Fig. 6 shows the behavior of H_s at the sensors, where the WG1 sensor behind the mangrove patch recorded greater values of H_s with the PETRA simulations (i.e. without mangroves) than the data measured in the field. In contrast, for sensor WG2 the greatest values correspond to those measured in the field, meaning that shoaling affects the PETRA simulations. This shows the direct effect of vegetation on H_s evolution when using a practical model.

The mean values of H_s calculated with the PETRA model are 0.07 m at WG1 and 0.065 m at WG2, which contrast with the mean values of H_s measured in the field (0.06 m and 0.08 m, respectively). This difference, using the PETRA model, represents an increase in H_s of 16.7% at WG1 and a decrease of 18.7% at WG2. This means that the combined effect of the bottom and vegetation decreases the H_s by 16.7% at WG1.

4. Discussion

This work presents the different results obtained by calculating C_D values as a function of incident flow. It also discusses their application to practical models, the use of a constant C_D value vs C_D values as a function of sea states to calculate energy flux and dissipation coefficients, and a comparison with the PETRA model.

Our results show an inverse relationship between the R_e number and C_D when using Mazda's method. Although we found that this relationship applied to *R. mangle* trees, other studies have found similar results for other mangrove species (see Table 2). Mazda et al. (1997b) recorded the same inverse relationship using field data from mangrove patches dominated by *Bruguiera gymnorrhiza* and *R. stylosa*. For both mangrove types, the C_D reached values between 0.4 and 10. It was shown that in shallow waters and swamps, the dense vegetation plays an important role in flow behavior. The values of R_e found in both sites ($0.5<9.0 \times 10^4$) were one order of magnitude lower than the results recorded in our study ($3.5<7.3 \times 10^5$). Our results also showed a higher flow velocity than that found by Mazda et al. (1997b) in the aforementioned mangroves, probably because their mangrove location was protected from the direct impact of incident waves. The main hydrodynamic effect found in their work was due to tides, which gave velocity values from >0.04 to 0.04 m/s and water levels of less than 0.3 m. In contrast, our mangrove patch is located in front of the transformed

Table 2
Overview of the results of previous studies into wave attenuation in vegetation vs our results.

Vegetation type > Location	R_e range	Velocity range	C_D range
Bruguiera gymnorrhiza from Nakama-Gawa on Iriomote Island (Japan), and *R. stylosa*, on Coral Creek (Hinchinbrook Island, Australia) (Mazda et al., 1997b)	$0.5<9.0\times10^4$	>0.04<0.04 m/s	0.4<10
SWAN model user guide suggestions based on Mendez and Losada (2004) using *Laminaria hyperbore*			0.09<6.90
Laboratory data for the parameterized *R. apiculata* (Husrin and Oumeraci, 2009)	$2.0<4.5\times10^4$		0.65<3.0
Laboratory models and field data recorded for the salt marsh species *Spartina alterniflora* and *Juncus roemerianus* (Ozeren et al., 2009)	$0.2<4.5\times10^3$		0.7<9.2*
Coastal wetlands in general (Hu et al., 2014a)	$0.2<5\times10^3$		0.5<4.8*
R. mangle patch from Islas del Rosario (Colombia) (present work)	$3<7.35\times10^5$	0.1<0.4 m/s	0.8<8.0

*Approximate values.

sea waves, as the study site is in a post-breaking zone. In addition, the two studies also showed contrasting values of H_s. While in Australian mangroves, the water level was between 0.1 m and 0.25 m, in the present study the values oscillated between 0.07 m and 0.11 m at WG2. Therefore, considering the form of equation 10 and according to the mean velocity values obtained, the values of C_D calculated in both studies are directly proportional to the H_s gradient and inversely proportional to flow velocity.

Despite the fact that Husrin and Oumeraci (2009) carried out an experimental study placing mangroves along a sand beach facing the incident waves, the laboratory data for the parameterized *R. apiculata* data also recorded lower values of R_e ($2.0<4.5\times10^4$) than those present in this work. However, the values of C_D recorded by Husrin and Oumeraci (2009) decreased from 3.0 to 0.65 as the R_e increased. The present study may differ due to the different physical configuration of the experiments, such as the arrangement of cylinders of known height and diameter, the scale, and the maximum values set to evaluate the vegetation response to tsunamis. Therefore, it can be said that the C_D values depend on the field and seasonal conditions where the mangroves grow. In addition, the R_e obtained in our study (with values between $3.5<7.3\times10^5$) was two orders of magnitude greater than that obtained by the laboratory models and field data recorded by Ozeren et al. (2009) for the salt marsh species *Spartina alterniflora* and *Juncus roemerianus* ($0.2<4.5\times10^3$). The same can be said for values recorded by Hu et al. (2014) for coastal wetlands in general ($0.2<5\times10^3$). In the latter case, the C_D was calculated for regular and irregular waves and for current-wave flow analysis using coastal wetland models in the laboratory. The differences between our results and some of the aforementioned studies are predictable considering the lower force exerted by non-woody species when compared to woody vegetation.

Like in the present work, Mazda et al. (1997b) used woody vegetation in the field for their study. The most important difference between their study and ours is related to the velocity values. In this work, the velocity values (between 0.1 and 0.4 m/s) were calculated using an approximation of the velocity spectrum, employing the free wave surface and pressure spectrum. This method can generate errors so it is important in future work to measure the incident velocity towards the mangroves and compare it with the method used here. The values of velocity recorded in this study are higher than those measured by Mazda et al. (1997b), probably due to the location of the two studies and the different wave dynamics.

In all cases shown in Table 2, the C_D decreases as the R_e increases (Mazda et al., 1997b; Mendez and Losada 2004; Husrin and Oumeraci 2009; Ozeren et al., 2009; Hu et al., 2014a), which means that the mangrove vegetation is more effective at dissipating wave energy under the effect of low energy sea waves than high energy ones.

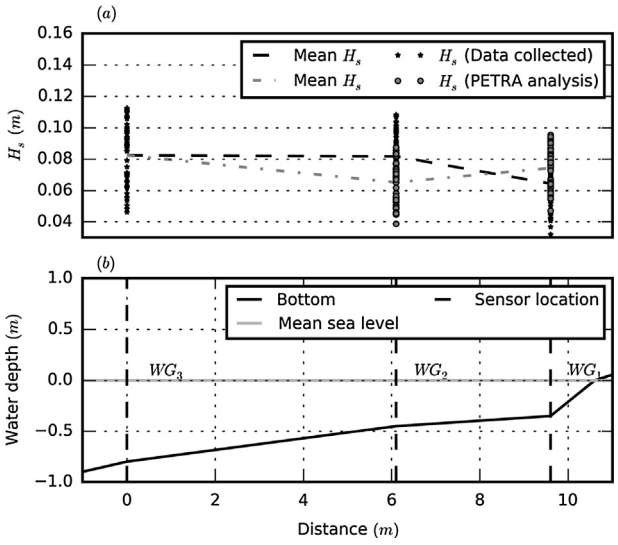

Fig. 6. Hs evolution (Measured data vs PETRA results).

Practical models use a constant and calibrated value of C_D. For example, the SWAN model user guide suggests values of C_D between 0.09 and 6.90, which are in contrast with the values found in the present work (between 0.8 and 8.0). Such differences are probably because the user guide is based on the results of Mendez and Losada (2004) using *Laminaria hyperbore*, a marine algae whose structural configuration is different to that of mangrove vegetation. Thus, the difference in the maximum C_D values between the SWAN model and our results is 15.2% and with the mean C_D values the difference is 28.5%. The difference is also caused by the bathymetry of our study zone and the nonlinear process in the wave<vegetation interaction. This means that the range of C_D values suggested by the SWAN model may be lower than the real C_D values and indicates that hydrodynamics in mangrove swamps may change according to the configuration of the mangrove species, the local bathymetry and the incident sea waves. Therefore, an error may be generated when the user calculates the value of dissipation by mangrove vegetation because the values of a constant C_D can underestimate the real ones, as is shown by the difference between the suggested values of the SWAN model and our results. Since with the SWAN model the user can chose a constant value of C_D, it is necessary to have knowledge of the vegetation type and its behavior for each sea state.

Suzuki et al. (2012) used the SWAN model with data collected by Vo-Luong and Massel (2008) for a mixed mangrove forest in Can Gio (South Vietnam). They also included the Keulegan-Carpenter number in the calibrated model and used *Laminaria hyperbore* to

calculate the C_D (Mendez and Losada, 2004), which reached values between 0.0 and 1.0. In the study by Suzuki et al. (2012), C_D is a function of the mean root diameter, the relative depth of the roots, the wave flow velocity and the peak period. In contrast, in our study using field data, C_D is a function of R_e and the characteristic length (L_e) of the mangrove patch. The fluctuations in C_D values highlight the importance of including the vegetation type in the model when using both field and laboratory data. This must happen before using the SWAN model or any other formulation.

Our results suggest that for a better approximation of these models, the C_D value needs to be calibrated according to both vegetation types and the physical conditions of the study site. It could be also interesting, as a first approximation, to create R_e vs. C_D plots for each type of vegetation in order to obtain a standardized method and evaluate the effective resistance of each vegetation type to different sea wave events. This approximation could contribute to the understanding of other important factors that affect the C_D value, such as water depth, the influence of the vegetation geometry and the influence of tides and sea waves separately. The results obtained by Husrin and Oumeraci (2009) and Mazda et al. (1997b), along with ours, could be used as a first approach for assessing the response of *Rhizophora* trees to such factors, taking into account the definition of the C_D value for each sea state.

Using a constant value of C_D, errors can be generated in the estimation of mangrove dissipation because, as shown by our results, C_D depends on the water surface gradient (I) and the incident velocity (Eq. (12)). These variables change over time for each sea state, generating a mangrove patch response as a function of the energy flow intensity, i.e. as a function of high and low wave energy and current velocities. Therefore, where C_D is calculated for each sea state, our results show that the behavior of the mangrove patch changes for each sea state.

Several authors relate the C_D values with the R_e number to represent the incident sea wave conditions (Mazda et al., 1997a,b; Mendez and Losada, 2004; Husrin and Oumeraci 2009; Ozeren et al., 2009; Hu et al., 2014a). This means that with a variation in flow conditions, the vegetation response will vary too. Therefore, to analyze the dissipation values that exceed a sea state over time (like time with constant flow conditions), we must consider that the C_D values change as variables like H_s and T_p change, as shown in the present work. However, mangroves are generally located in swamps where the most significant flow variation is caused by the influence of tides. Therefore, during low and high tides (where the frequency is almost constant) the variation in C_D values is not significant.

By comparing the mean values of H_s in this work for each gauge we can conclude that the reduction in the percentage of significant wave height between WG3 and WG1 ($H_{s3>1} = H_{s3}/H_{s1}$) is 33.33% and between WG2 and WG1 ($H_{s2>1} = H_{s2}/H_{s1}$), where the presence of vegetation is the most important physical barrier, it is 25%. Therefore, the combined effect of the slope and vegetation is around 75% ($H_{s2>1}/H_{s3>1}$) of the total significant wave height reduction. The wave dissipation across coastal vegetation was reordered by different authors based on the vegetation length scale (L_e) and the total size of the vegetation zone. Möller et al. (1999) presented a mean wave dissipation percentage of 60.96% for salt marshes (including species such as *Suaeda maritima, Puccinellia maritima, Halimione portulacoides, Armeria maritima, Aster tripolium, Limonium vulgare, Salicornia spp., Spartina anglica*) and 15.29% for sand flats 200 m long in front of existing sea defense lines in North Norfolk, England. The difference is based on the size of the vegetation zones, mainly the length of vegetation that the sea waves cross. Our results and the results of Möller et al. (1999) show how important the role of vegetation structures is in coastal setback/shoreline realignment schemes. In the particular case of the Colombian coast, it is necessary to investigate the hydrodynamics of mangrove swamps, including both physical and biological parameters, in order to include ecological engineering in coastal management plans.

Besides the wave dissipation percentage, the effect of vegetation on the wave flow can be analyzed by the transference of energy between two known points. Mendez and Losada (2004) developed a parametric equation to quantify the energy dissipated by vegetation. In their work, the values of C_D were calibrated using *Laminaria hyperbore,* and the parametric equation was used with C_D values calculated by Mazda's method. In addition, the dissipation energy produced by breaking was used in both studies with the parametric equation of Alsina and Baldock (2007). The energy flux as a function of bottom and vegetation dissipation gives information about the nonlinear process in the study zone, showing the percentage not explained by the linear sum of only two effects. The comparison made in our work cannot explain the 9.6% difference between energy flux and the sum of parameterized coefficients. This shows how the main process between WG2 and WG1 is a product of the effect of vegetation and the bottom. Furthermore, it demonstrates the presence of other physical processes, like refraction, shoaling and viscosity, as mentioned before (Section 2.1). In this case, these processes represent less than 10% of the total wave energy dissipation. All physical processes must be discriminated and included in future studies to obtain 100% of the energy flux behavior and show the effect of isolated vegetation. In this way, the contribution of each physical process involved in the total values of wave dissipation around the mangrove patch can be discretized.

Likewise, the results based on the calculated C_D differ from those obtained with constant values of C_D. The differences, presented in Fig. 5, show two important aspects in the calculation of energy dissipation by vegetation and energy flux. The first is the importance of considering a suitable value of C_D, because with the suggested values in two cases the D_{veg} was overestimated (74.8% and 246.6%) and in one case it was underestimated (30.1%). Therefore, none of the three cases (C_D = 0.06, 3.48 and 6.90) could explain a 90.4% energy flux, as in the case of D_{veg} with calculated and non-constant C_D values. The second important aspect, which is rather difficult to implement in numerical models, is the calculation of D_{veg} based on C_D for each sea state. Each sea state was analyzed under different flow conditions, which was important in representing the non-steady flow between the different sea states through measurements or simulation series. This difference shows that the C_D value and all variables involved in the parametric equations for the vegetation and the bottom, as well as other physical processes presented in the literature, need to be calculated (Mendez and Losada, 2004; Alsina and Baldock, 2007). The results obtained with the aforementioned equations can only be validated and compared for each study zone according to their main variables, such as C_D.

Therefore, thorough and rigorous fieldwork should be carried out in a mangrove forest. It is also necessary to gather more field data of the coastal geomorphology and additional wave conditions in the study zone. In this way, other methodologies to obtain accurate C_D and energy dissipation values caused by further physical processes can be explored, evaluated and applied. The quantitative contributions of mangrove forests as coastal protection environments can then be identified. This information would be valuable for the management and protection of coastal ecosystems using mangroves. At the same time, this study could be improved by the collection and inclusion of additional field data in numerical models, such as incident velocity, the flow force across mangrove swamps and geometric characteristics of different mangrove types.

To differentiate the bottom effect from the combined bottom<vegetation effect, the PETRA model (González et al., 2004) was used. The particular behavior measured in WG2 showed the mangrove patch as an obstacle, generating a higher sea level than the PETRA model (Fig. 6). In WG1, the measured values (which contain information about the combined bottom<vegetation effect)

were 16.7% lower than values obtained by the PETRA model (with information about the bottom effect), showing a greater dissipation of incident sea waves. Furthermore, in WG1 the case using mangroves obtained lower values of H_s than the case without mangroves. Therefore, the effectiveness of mangroves at reducing the energy flux and the values of H_s should be studied for all mangrove forests, employing more sensors to define the energy flux over a sea level profile.

5. Conclusions

As was shown in this work, the real C_D value depends on geometric characteristics of vegetation and incident sea wave conditions over time, i.e. for each sea state. The values of C_D were from 0.98 to 7.95, taken over 57 h with mean sea waves. Therefore, as a first approximation, this experimental work shows the variability in C_D over time, which affects the parametric equations used to calculate the dissipation rate due to the *R.* mangrove patch. This means that with a variation in flow conditions the response of the vegetation will vary too.

Furthermore, the C_D variability over time can explain that 90.4% of total energy flux is due to the effect of the bottom and vegetation. The other 9.6% may correspond to physical processes like refraction, reflection and shoaling that have a smaller influence on the dissipation process.

With the use of the PETRA model, we can conclude that the presence of vegetation is important in the physical process of dissipation. As a result, coastal ecosystems need to be protected, and we need to know how the flow evolves through these ecosystems and determine the mean and maximum conditions for a functional structure design.

Acknowledgments

The authors are grateful to COLCIENCIAS and the projects “Extreme Oceanic Events in Colombian Pacific and Caribbean Insular Coastal Ecosystems (Eventos Oceánicos Extremos en Ecosistemas Costeros Insulares del Pacífico y el Caribe Colombianos)” and “Study of Wave Dissipation in Natural Structures and their Response to Extreme Events” (Estudio de la disipación del oleaje en estructuras naturales y su respuesta ante eventos extremos) for their financial support. We are also grateful to the Hydraulic Laboratory Jairo Murillo V. of Universidad Nacional de Colombia Sede Medellin and especially to Andrea Galeano for her assistance in the field.

References

Alsina, J.M., Baldock, T.E., 2007. Improved representation of Breaking wave energy dissipation in parametric wave transformation models. Coastal Eng. 54 (10), 765–769, http://dx.doi.org/10.1016/j.coastaleng.2007.05.005.

Anderson, Mary E, Mckee Smith, Jane, Kyle Mckay, S., 2011. Wave Dissipation by Vegetation (no. September).

Aswani, Shankar, Christie, Patrick, Muthiga, Nyawira a., Mahon, Robin, Primavera, Jurgenne H., Cramer, Lori a., Barbier, Edward B., et al., 2012. The way forward with ecosystem-based management in tropical contexts: reconciling with existing management systems. Marine Policy 36 (1), 1–10, http://dx.doi.org/10.1016/j.marpol.2011.02.014.

Augustin, Lauren N., Irish, Jennifer L., Lynett, Patrick, 2009. Laboratory and numerical studies of wave damping by emergent and near-emergent wetland vegetation. Coastal Eng. 56 (3), 332–340, http://dx.doi.org/10.1016/j.coastaleng.2008.09.004 (Elsevier B.V.).

Battjes, J.A., Janssen, J., 1978. Energy loss and set-up due to breaking of random waves. Coastal Eng. Proc. 1, http://dx.doi.org/10.1002/cbdv.200490137/abstract (http://onlinelibrary.wiley.com).

Booij, N., Ris, R.C., Holthuijsen, L.H., 1999. A third-generation wave model for coastal regions: 1. model description and validation. J. Geophys. Res. 104 (C4), 7649.

Chatenoux, Bruno, Peduzzi, Pascal, Scientific Report, Unep Asian, Tsunami Disaster, and Task Force, 2005. Analysis on the Role of Bathymetry and Other Environmental Parameters in the Impacts from the 2004 Indian Ocean Tsunami (no. June).

Dalrymple, R.A., Dean, R.G., 1984. Water Wave Mechanics for Engineers and Scientists (http://www.asianscientist.com/books/?book=1232).

Dalrymple, Robert A., Asce, M., Kirby, James T, 1984. Wave diffraction due to areas. J. Waterway, Port, Coastal, Ocean Eng. 110 (1), 67–79.

González, M., Medina, R., Osorio, A., Lomónaco, P., 2004. Sistema de Modelado Costero Español (SMC). . . . de Hidráulica, São Pedro, Estado De., http://dx.doi.org/10.13140/RG.2.1.2105.0405 (no. OCTOBER 2004).

Horstman, E.M., Dohmen-Janssen, C.M., Narra, P.M.F., van den Berga, F., Siemerink, M., Hulscher, S.J.M.H., 2014. Wave attenuation in mangroves: a quantitative approach to field observations. Coastal Eng. 94, 47–62, http://dx.doi.org/10.1016/j.coastaleng.2014.08.005 (Elsevier B.V.).

Hu, Zhan, Suzuki, Tomohiro, Zitman, Tjerk, Uittewaal, Wim, Stive, Marcel, 2014. Laboratory study on wave dissipation by vegetation in combined current wave flow. Coastal Eng. 88, 131–142, http://dx.doi.org/10.1016/j.coastaleng.2014.02.009 (Elsevier B.V.).

Huang, Zhenhua, Yu, Yao, Shawn, Y. Sim, Yao, Yao, 2011. Interaction of solitary waves with emergent, rigid vegetation. Ocean Eng. 38 (10), 1080–1088, http://dx.doi.org/10.1016/j.oceaneng.2011.03.003 (Elsevier).

Hui, Er-qing Erqing, Hu, Xing-e, Jiang, Chun-bo, Ma, Fang-kai, Zhu, Zhen-duo, 2010. A study of drag coefficient related with vegetation based on the flume experiment. J. Hydrodyn. Ser. B. 22 (3), 329–337, http://dx.doi.org/10.1016/S1001-6058(09)60062-7 (Publishing House for Journal of Hydrodynamics).

Husrin, Semeidi, Oumeraci, Hocine, 2009. Parameterization of Coastal Forest Vegetation and Hydraulic Resistance Coefficients for Tsunami Modelling., pp. 78–86 (http://scholar.google.com/scholar?hl=en&btnG=Search&q=intitle:Parameterization+of+Coastal+Forest+Vegetation+and+Hydraulic+Resistance+Coefficients+for+Tsunami+Modelling#0.).

Husrin, Semeidi, Strusinska, Agnieszka, Oumeraci, Hocine, 2012. Experimental study on tsunami attenuation by mangrove forest. Earth Planets Space 64 (10), 973–989, http://dx.doi.org/10.5047/eps.2011.11.008.

Iimura, Kosuke, Tanaka, Norio, 2012. Numerical simulation estimating effects of tree density distribution in coastal forest on tsunami mitigation. Ocean Eng. 54 (November), 223–232, http://dx.doi.org/10.1016/j.oceaneng.2012.07.025 (Elsevier).

Jimenez, Jorge A., 1980. Rhizophora Mangle L. Red Mangrovee. *ITF-SM-2*. U.S. Department of Agriculture, Forest Service, Southern Forest Experiment Station, New Orleans, LA.

LEMA, Á., 2003. Elementos Teórico-Prácticos Sobre Inventarios Forestales: Estadística Y Planeación. Universidad Nacional de Colombia, Sede Medellín, Medellín, Colombia.

Lewis, Roy R., 2005. Ecological engineering for successful management and restoration of mangrove forests. Ecol. Eng. 24 (4), 403–418, http://dx.doi.org/10.1016/j.ecoleng.2004.10.003.

Möller, I., Spencer, T., French, J.R., 1999. Wave Transformation over Salt Marshes: A Field and Numerical Modelling Study from North Norfolk, England, *Estuarine, Coastal and* . . ., 411<26. http://www.sciencedirect.com/science/article/pii/S0272771499905097.

Maza, Maria, Lara, Javier L., Losada, Inigo J., 2015. Tsunami wave interaction with mangrove forests: a 3-D numerical approach. Coastal Eng. 98 (April), 33–54, http://dx.doi.org/10.1016/j.coastaleng.2015.01.002 (Elsevier B.V.).

Mazda, Yoshihiro, Magi, M., Kogo, M., Hong, P.N., 1997a. Mangroves as a coastal protection from waves in the Tong King Delta, Vietnam. Mangroves Salt Marshes 1, 127–135, http://dx.doi.org/10.1023/A:1009928003700.

Mazda, Yoshihiro, Wolanski, Eric, King, Brian, Sase, Akira, Ohtsuka, Daisuke, Magi, Michimasa, 1997b. Drag force due to vegetation in mangrove swamps. Mangroves Salt Marshes 1, 193–199, http://dx.doi.org/10.1023/A:1009949411068.

Mazda, Yoshihiro, 2014. Outline of the Physical Processes Within Mangrove Systems., pp. 1–63.

Mendez, Fernando J., Losada, Inigo J., 2004. An empirical model to estimate the propagation of random breaking and nonbreaking waves over vegetation fields. Coastal Eng. 51 (2), 103–118, http://dx.doi.org/10.1016/j.coastaleng.2003.11.003.

Morison, J.R.J., Johnson, W., Schaaf, S.A., 1950. The force exerted by surface waves on piles. J. Petrol. Technol. 2 (5), Society of Petroleum Engineers: 149<54.

Noarayanan, L., Murali, K., Sundar, V., 2012. Manning's 'n' co-efficient for flexible emergent vegetation in tandem configuration. J. Hydro-Environ. Res. 6 (1), 51–62, http://dx.doi.org/10.1016/j.jher.2011.05.002 (Elsevier B.V).

Osorio, Andrés F., Montoya, Rubén D., Carlos Ortiz, Juan, Peláez, Daniel, 2016. Construction of synthetic ocean wave series along the colombian caribbean coast: a wave climate analysis. Appl. Ocean Res. 56 (March), 119–131, http://dx.doi.org/10.1016/j.apor.2016.01.004 (Elsevier B.V).

Ozeren, Y., Asce, A.M., Wren, D.G., Asce, M., Wu, W., 2009. Experimental Investigation of Wave Attenuation Through Model and Live Vegetation., pp. 1–12, http://dx.doi.org/10.1061/(ASCE)WW.1943-5460.0000251.

Robertson, A.I., Alongi, D.M., 1992. Tropical Mangrove Ecosystems.

Suárez, July A, Ligia E Urrego, Andrés Osorio, and Hiara Y Ruiz. 2015. Oceanic and Climatic Drivers of Mangrove Changes in the Gulf of Urabá, Colombian Caribbean/Controladores Oceánicos Y Climáticos de Cambios En Los Manglares En El Golfo de Urabá, Caribe Colombiano. *Latin American Journal of Aquatic Research* 43 (5). Pontificia Universidad Católica de Valparaíso: 972.

Suzuki, Tomohiro, Zijlema, Marcel, Burger, Bastiaan, Meijer, Martijn C., Narayan, Siddharth, 2012. Wave dissipation by vegetation with layer schematization in

SWAN. Coastal Eng. 59 (1), 64–71, http://dx.doi.org/10.1016/j.coastaleng.2011.07.006 (Elsevier B.V.).
Svendsen, I.A., 2006. Introduction to Nearshore Hydrodynamics (http://scholar.google.com/scholar?hl=en&btnG=Search&q=intitle:iNTRODUCTION+TO+NEARSHORE+HYDRODYNAMICS#0).
Vo-Luong, Phuoc, Massel, Stanislaw, 2008. Energy dissipation in non-uniform mangrove forests of arbitrary depth. J. Mar. Syst. 74 (1<2), 603–622, http://dx.doi.org/10.1016/j.jmarsys.2008.05.004 (Elsevier B.V.).
Yáñez-Arancibia, A., John, W.D., Robert, R.T., Richard, H.D., 2010. Los Manglares Frente Al Cambio Climático ¿tropicalización Global Del Golfo de México? JOUR. Impactos Del Cambio Climático Sobre La Zona Costera. Instituto de Ecología AC (INECOL), Texas Sea Grant Program. Instituto Nacional de Ecología (INE-SEMARNAT), México.